

# 3D lithography by rapid curing of the liquid instabilities at nanoscale

Simonetta Grilli, Sara Coppola, Veronica Vespini, Francesco Merola, Andrea Finizio, and Pietro Ferraro<sup>1</sup>

Consiglio Nazionale delle Ricerche Istituto Nazionale di Ottica—Sezione di Napoli, Via Campi Flegrei, 34—80078 Pozzuoli (Naples), Italy

Edited by T. C. Lubensky, University of Pennsylvania, Philadelphia, PA, and approved August 1, 2011 (received for review July 6, 2011)

**In liquids realm, surface tension and capillarity are the key forces driving the formation of the shapes pervading the nature. The steady dew drops appearing on plant leaves and spider webs result from the minimization of the overall surface energy [Zheng Y, et al. (2010) *Nature* 463:640–643]. Thanks to the surface tension, the interfaces of such spontaneous structures exhibit extremely good spherical shape and consequently worthy optical quality. Also nanofluidic instabilities generate a variety of fascinating liquid silhouettes, but they are however intrinsically short-lived. Here we show that such unsteady liquid structures, shaped in polymeric liquids by an electrohydrodynamic pressure, can be rapidly cured by appropriate thermal treatments. The fabrication of many solid microstructures exploitable in photonics is demonstrated, thus leading to a new concept in 3D lithography. The applicability of specific structures as optical tweezers and as novel remotely excitable quantum dots—embedded microresonators is presented.**

A wide variety of lithographic techniques have been developed for fabricating 3D structures (1–5), such as soft lithography (6) that allows one to develop lab-on-chip devices with applications ranging from organic light emitting diode to biology and biochemistry (7). Among others, “capillary-force lithography” is able to nicely pattern polymers at nano-/microscale, but with a very low aspect ratio, in a single step and avoiding the use of external forces (8). Other approaches generate self-patterned structures by using destabilizing forces produced by electric fields, namely electrohydrodynamic (EHD) lithography (9). In EHD lithography, amazing polymeric patterns have been reported, demonstrating the possibility of controlling the process with high accuracy. This method appears suitable only for a few types of periodic patterns having a relatively low aspect ratio (i.e., pillars, dots, and lines). In fact, the control of liquid film instabilities is a demanding task as very little perturbations could drag the nanofluidic system toward nonfully predictable configurations. Such occurrence, for high aspect-ratio features, would prevent the achievement of the expected final steady state. The EHD lithography is usually performed at temperatures above the glass transition of the polymer film [typically polystyrene or poly(methyl methacrylate)], obtaining permanent microstructures by slow annealing and successive cooling, taking hours (10–13).

In general, the hydrodynamic techniques produce steady-state structures resulting from the equilibrium state of a specific fluidic effect. Conversely, the core of our approach consists in “rapid-curing” temporary structures, which evolve continuously under specific fluidic instabilities, by a fast heating procedure. The interesting aspect of this approach is that it gives access to very intriguing fluid shapes, occurring in unsteady fluid physics at nanoscale, which could be very useful in modern science. As investigated recently, breakup of viscoelastic filaments passes through the formation of temporary pearls interconnected by a thin thread, the so-called beads-on-a-string (BOAS) structures (12–14). So a question arises: Is it possible to mimic nature and produce in a controlled way liquid instabilities and stop their “evolution history,” driven by the physics laws? Or, with a popular analogy, is it possible to “freeze” nanofluidic instabilities in polymers as occurs for iced fountain’s jets or the waterfalls in a cold winter?

Here we show a unique but straightforward approach that exploits instabilities and self-assembling of polymeric liquids for fabricating single or arrays of complex high aspect-ratio 3D microstructures. Liquid instabilities are first driven via EHD pressure and then quickly cured to obtain permanent 3D microstructures, by the same thermal treatment, paving the way to a previously undescribed paradigm in fabrication of 3D polymer microstructures. The fabrication of polymer wires, needles, pillars, cones, or microspheres is reported. The polymer structure functionalization through nanoparticles is also shown, and practical proofs of its use in photonics are presented.

## Design and Working Principle of the Technique

Our polydimethylsiloxane (PDMS) structures are fabricated through liquid instabilities induced by surface EHD pressure that can commonly be adopted in EHD lithography, in electrospinning processes (15–17) or in a unique approach named pyro-EHD (PEHD) (18). It is important to note that, to the best of our knowledge, EHD or electrospinning has never been used for building up 3D microstructures such as those reported here, having high aspect ratios compared to those obtained through EHD or capillary-force lithography (8, 9).

In our method the air–liquid interface is subjected to an EHD field able to increase the dominant instability, among the natural spectrum of capillary surface waves, at room temperature, without a preliminary annealing process (9). The polymeric permanent structures are generated in our case by rapid cross-linking, which allows us to reduce the overall process duration from hours, required for the glass transition, down to seconds. The combination of high viscosity (12) and rapid cross-linking of PDMS allows us to fabricate structures with aspect ratios extraordinary higher, up to three orders of magnitude, compared to those reported in previous articles (8–10, 19). In fact, the typical aspect-ratio values reported in previous works are in the range of 0.29–0.83, whereas up to 186 is reached here.

The experimental configuration adopted in this work consists basically of a glass slide supporting a sessile nanodrop as liquid reservoir, facing a lithium niobate (LN) substrate at distance  $D$ . Any temperature change  $\Delta T$  of LN causes a variation  $\Delta P_s$ , which builds up electric charges: The resulting electric field is able to exert an EHD force on the liquid PDMS creating a liquid bridge across the two substrates, as shown in Fig. 1 *A–F* (see *Methods*). The EHD pressure and fluid dynamics cause liquid depletion from the bridge and consequent formation of various temporary liquid silhouettes (12) having the inevitable fate toward the collapsing point (see *Movie S1*).

Author contributions: S.G., S.C., V.V., and P.F. designed research; S.G., S.C., V.V., F.M., and A.F. performed research; S.G., S.C., V.V., F.M., A.F., and P.F. contributed new reagents/analytic tools; S.G., S.C., V.V., F.M., A.F., and P.F. analyzed data; and S.G. and P.F. wrote the paper.

The authors declare no conflict of interest.

This article is a PNAS Direct Submission.

<sup>1</sup>To whom correspondence should be addressed. E-mail: [pietro.ferraro@ino.it](mailto:pietro.ferraro@ino.it).

This article contains supporting information online at [www.pnas.org/lookup/suppl/doi:10.1073/pnas.1110676108/-DCSupplemental](http://www.pnas.org/lookup/suppl/doi:10.1073/pnas.1110676108/-DCSupplemental).



focused onto the microstructures by a parabolic mirror. The temperature of the curing process was about 130 °C.

With the aim to assure that the curing process was fully accomplished, we performed some tests. As shown in Fig. 1J a wire with beads can be elongated up to about 100% of its length. A further example is shown in Fig. 1K where a cured wire with multiple beads, obtained as demonstrated in Movie S4, is also elongated and then compressed to demonstrate the complete curing of the structure without breaking.

In Fig. 2A and B the schematic view of the PDMS patterns (dots and strips) used as reservoirs are shown. Fig. 2C and D shows the top and side microscope images of permanent symmetric bridges obtained by rapid curing of the stationary state. The microsized structures displayed in Fig. 2C and D–H are formed using the packaged configuration with  $d$  ranging from 150 to 500  $\mu\text{m}$  and printed separate drops of PDMS as reservoirs. The figures present the top and the side microscope images of permanent symmetric bridges with different aspect ratios, obtained through the rapid curing of the stationary state corresponding to scenario (1). The sample having the LN above the package and in direct contact with the thermal source was heated onto a hot plate at 150 °C for 120 s, activating the PEHD effect and realizing the rapid curing. Two-dimensional arrays of wired

structures, where the PDMS included dispersed multiwalled carbon nanotubes (MWCNTs), are reported in Fig. 2E. PDMS, diluted with hexane (mixing ratio 3 : 1) and with dispersed carbon nanotubes (multiwalled, diameter 110–170 nm, length 5–9  $\mu\text{m}$ , Aldrich Chemistry), was patterned as an array of separate drops. In this case the hot-air jet was used for triggering the nanofluidic PEHD instability as well as for the rapid curing of the structures, in the same conditions described in Fig. 1. The use of MWCNTs makes the curing process faster when compared to the rapid cross-linking using just pure PDMS. The experimental characterization of the curing speed shows an increase of about 25%. This improvement was estimated by testing a sequence of drops with and without dispersed carbon nanotubes. The drops were placed on a glass side and were heated by the hot-air jet for a specific time and the curing stage was checked. In this case a hot-air jet was used for triggering the nanofluidic pyro-EHD instability as well as for the rapid curing of the structures. Conical structures with needle tips, obtained by rapid curing of the Taylor's cone, are shown in Fig. 2F. Essentially such structures consist of two facing cones with different apex angles connected by a thin wire. Fig. 2F shows the conical structures (Taylor's cone) with and without the needle tip formed onto the receiving substrate obtained by unwrapping the package configuration of Fig. 2E.

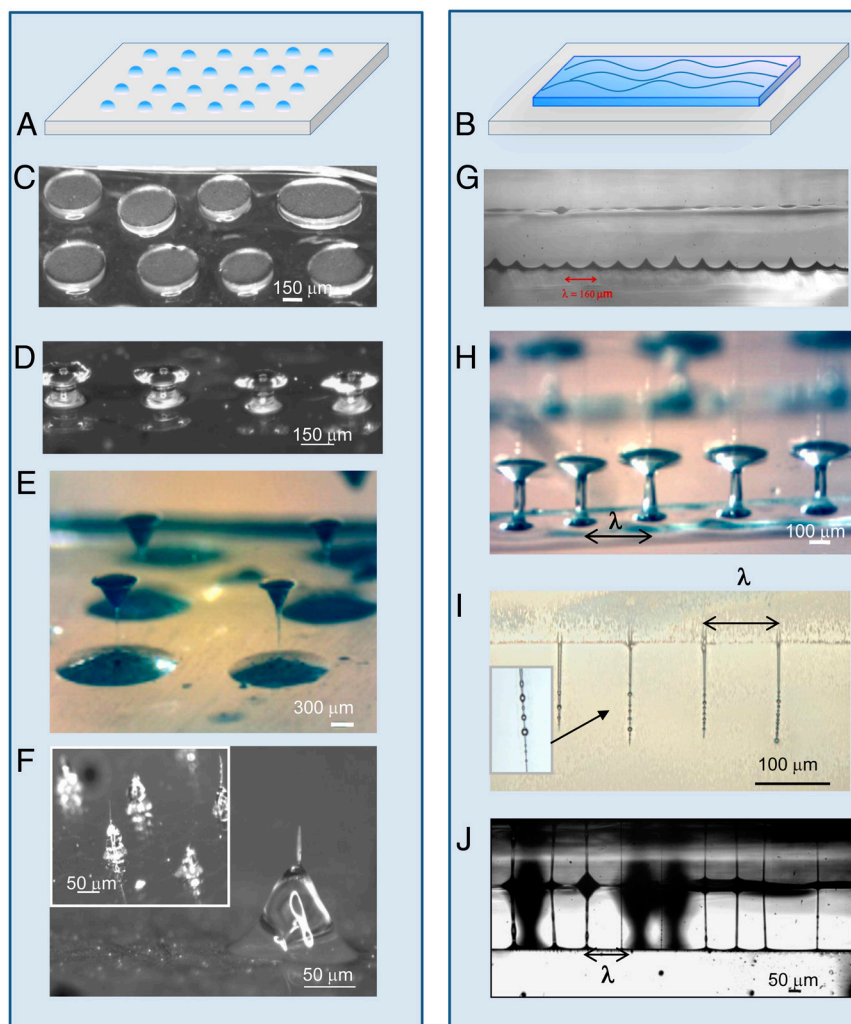


**Fig. 2.** Structures obtained with patterned reservoirs droplets and films. (A and B) Schematic view of two typical reservoir geometries consisting of arrays of single drops and aligned strips of PDMS, respectively. (C and D) Soft solid-like bridges with different aspect ratios (0.36 and 0.88, respectively). (E) Solid-like wired structures connected by conical terminations. (F) Conical structures with and without needle tip. (G) Self-assembled multiple jets. (H) Array of bridges obtained from PDMS strips including MWCNT to improve the heat diffusion into the polymer. (I) Extended focus image of the cured BOAS structures and large and magnified view of another cured BOAS structure. (J) Side view of periodic solid-like wires. The aspect ratio is around 60.



with the film of PDMS is then placed on a hot plate at a temperature of 115 °C for 10 min, generating a series of PDMS cones. By heating the sample, the film instability was produced and the rapid-curing process of the polymer allows for the formation of microaxicon structure. The lid of LN was then removed, leaving the microaxicon deposited on glass. An axicon is able to produce Bessel beams having high depth of focus when compared to focused Gaussian beams obtained by high numerical aperture microscope objectives (see details in *SI Text Section C*, Table S2, and Fig. S2). This is a clear advantage for optical trapping (i.e., for particles trapping by the light forces) compared to the use of microscope objectives. In fact, an axicon is very useful as optical tweezer for trapping and sorting microparticles or biological cells (20). Small dimensions of axicons could make these elements suitable for embedding them into lab-on-a chip devices, to image or to trap microobjects in microfluidic channels, unrealizable things with cumbersome microscope objectives having limited depth of field. We report here an optical tweezers experiment demonstrating application of the rapid cured PDMS axicons for single particle trapping (see *Movie S7*) and for high depth-

of-focus simultaneous multiple trapping in different planes along the *z* direction of six 10- $\mu$ m-sized latex particles (Fig. 3 *E* and *F* and *Movie S8*).

**Whispering Gallery Mode (WGM) Microresonators.** Microspheres may be used as resonators where the resonance modes, known as WGMs, arise from the confinement of light by total internal reflection. Refractive index changes can induce a resonance shift that is used for label-free detection of a single molecule or virus (21, 22). Recently, structures with local light sources have been proposed as microresonators remotely excitable, i.e., as *active* microstructures, by dye (23) or quantum dots (QDs) (24, 25), thus avoiding intimate contact between the resonator and the evanescent wave source for coupling light. The BOAS we fabricated may be used for sensing applications (26) and, as depicted in the outlook in Fig. 4A, either as *passive* or *active* resonators, because PDMS has demonstrated quality factors of  $10^6$  (27). Such microresonators do not require complex fabrication processes and the smooth surfaces are spontaneously given by the surface tension. As *active* elements, we successfully embedded CdSe/Zns core/

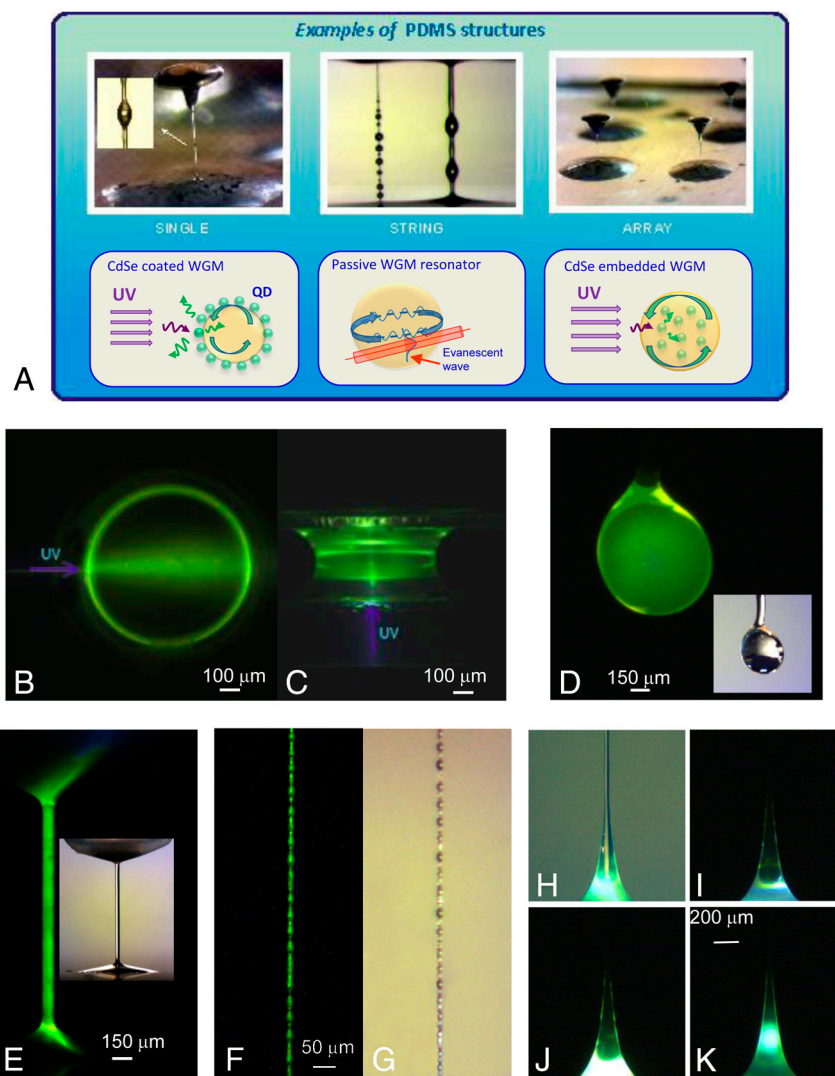


**Fig. 4.** Applicability of frozen PDMS structures as microresonators. (A) Outlook of the various potential resonator applications: classical evanescent field coupling (24, 25); WGMs from QD-infused structures (22); WGMs from QD-embedded structures (23). (B and C) Top and side views of the fluorescence image generated by a QD-embedded PDMS bridge. The arrows indicate the direction of the UV signal and the bright rings correspond to preferential WGMs. (D) Fluorescence image of a PDMS microsphere and the corresponding white light picture (*Inset*). The nearly homogeneous green emission is due to the isotropic signal of the dispersed QDs combined with the spherical symmetry of the structure. (E) Fluorescence image of a PDMS wire where the presence of preferential WGMs is evidenced by the bright walls. (*Inset*) The corresponding white light image. (F and G) BOAS with beads diameter around 10  $\mu$ m under UV and white light illumination. (H–K) Fluorescence images of conical structures.

shell QDs. Samples of degassed PDMS with CdSe QD nanocrystals were prepared by mixing 3 mL of PDMS with 300  $\mu\text{L}$  of Lumidots CdSe 590 nm (5 mg/mL concentration in toluene, fluorescence emission maxima spanning the visible spectrum, Sigma-Aldrich). The mixtures were obtained by vacuum-stirring in order to vaporize the solvent (toluene), making easier the curing process. A mixture droplet was placed on a glass slide and the auxiliary LN plate was mounted on independent vertical translation stages (separate configuration) to control the distance  $D$  while PDMS wire-structures were in progress. The curing process was obtained by a lamp as in case of Fig. 1J.

The fabricated 3D arranged beads can be remotely excitable without requiring distributed Bragg reflectors, as in case of the recent QD-embedded hemispherical structures in ref. 24. Fig. 4B and C shows the top and the side view, respectively, of the typical fluorescence effect induced into a QD-embedded frozen PDMS bridge, excited by a continuous-wave laser emitting at 325 nm. Bright rings along the rim of the bridge correspond to the formation of a preferential WGM due to the axial symmetry of the structure (26). The QD-embedded microsphere in Fig. 4D exhibits homogeneous photoluminescence. Fig. 4E shows the fluorescent image of a wire with uniform and stable photoluminescence during UV scanning (see Movie S9). Fig. 4F and G show QD-embedded BOAS excited by a UV lamp. In Fig. 4H–K the emission of conical structures during UV scanning is shown. The brighter regions in the periphery are attributed to resonant modes corresponding to different wavelength emissions (see Movie S10). Moreover, the well-known softness of PDMS would provide additional tuning functionality. In fact, as demonstrated in Fig. 1J and K, the cured microstructures can be mechanically stretched thus causing a change of the spherical shape. This is an important feature when WGM optical microresonators are applied for sensing purposes. Dynamic behavior can be nicely observed in Movies S3 and S4.

The fabrication process is easier to accomplish than other methods, where QDs are embedded into the periphery of polymer microspheres through complicated chemical procedures (24), enabling the inclusion of the QDs into deeper regions of the structures.

In conclusion, “Mother Nature” shapes liquid configurations during the evolution of liquid EHD instabilities, whereas a facile and rapid-curing process can produce microphotonic elements

—a sort of natural nanofluidic “optics foundry.” Multiphase structures are fabricated through the appropriate dispersion of solid particles into the PDMS layer. The ability to fabricate fibers with BOAS and diameter on the micrometer scale gives the opportunity to engineer scaffolds at microscale. Once the scaffold is created, using the rapid-curing process reported here, its surface could be useful for tissue engineering or drug delivery by functionalizing it (28), thus avoiding problems related to the high temperature required for during the fabrication process.

We believe that further theoretical investigations (12), in combination with the simple rapid-curing approach demonstrated here, will allow in the future the development of a previously undescribed “3D lithography concept/platform,” in which nanofluidic instabilities could be “fluidynamically” designed a priori with the aim at fabricating even more complex shapes exploitable in many fields.

## Methods

**Lithium Niobate Crystals.** The LN crystals used for the pyroelectric effect were z-cut single domain wafers optically polished on both sides (by Crystal Technology Inc.), with 3-inch diameter and 0.5-mm thickness.

**Heat Sources.** The hot-air gun, used for cross-linking rapidly the PDMS fluidic structures, had an operation temperature ranging from 50 to 660  $^{\circ}\text{C}$  (discrete steps of 10  $^{\circ}\text{C}$ ) and an air volume throughput in 10 stages between 250 and 500 L/min. The hot tip of a conventional soldering iron, used as a contact thermal stimulus for the pyroelectric effect, had a maximum operation temperature of 250  $^{\circ}\text{C}$ .

**The Pyroelectric Effect.** At equilibrium, the spontaneous polarization  $P_s$  of the LN crystals is fully compensated by the external screening charge and no electric field exists (29). When the crystal is subjected to a temperature variation  $\Delta T$ , the spontaneous polarization  $P_s$  varies and, neglecting the losses, an uncompensated surface charge  $\sigma = P_s \Delta T$  builds up. Therefore an electric field appears across the z surfaces. In case of LN at 25  $^{\circ}\text{C}$ , the pyroelectric coefficient  $P_c$  is equal to  $-8.3 \times 10^{-5} \text{ C}/^{\circ}\text{C}/\text{m}^2$ .

**Imaging Setup.** The illumination equipment consisted of a conventional blue collimated led (wavelength of 470 nm and beam power around 400 mW) equipped with a neutral density filter. A 5 $\times$  microscope objective was used for visualizing the PDMS instabilities onto a CMOS camera. The camera had a pixel area of  $(12 \times 12) \mu\text{m}^2$  and was able to capture 125 frame  $\text{s}^{-1}$  with a resolution of  $(1,280 \times 1,024)$  pixel $^2$ .

- Bowden N, Brittain S, Evans AG, Hutchinson JW, Whitesides GM (1998) Spontaneous formation of ordered structures in thin films of metals supported on an elastomeric polymer. *Nature* 393:146–149.
- Thangawong AL, Swartz MA, Glucksberg MR, Ruoff RS (2007) Bond detach lithography: A method for micro/nanolithography by precision PDMS patterning. *Small* 3:132–138.
- Piner RD, Zhu J, Xu F, Hong S, Mirkin CA (1999) “Dip-pen” nanolithography. *Science* 283:661–663.
- Stellacci F (2006) Towards industrial-scale molecular nanolithography. *Adv Funct Mater* 16:15–16.
- Wang L, Zhang D, Zhang H, Jiang JZ (2010) Fabrication of micropillars by laser-induced thermoplastic method. *Appl Phys Lett* 97:131905.
- Xia Y, Whitesides GM (1998) Soft lithography. *Annu Rev Mater Sci* 28:153–184.
- Park S, Huh YS, Craighead HG, Erickson D (2009) A method for nanofluidic device prototyping using elastomeric collapse. *Proc Natl Acad Sci USA* 106:15549–15554.
- Bruinink CM, et al. (2006) Capillary force lithography: Fabrication of functional polymer templates as versatile tools for nanolithography. *Adv Funct Mater* 16:1555–1565.
- Scaffer E, Thurn-Albrecht T, Russel TP, Steiner U (2000) Electrically induced structure formation and pattern transfer. *Nature* 403:874–877.
- Verma R, Ashutosh Sharma A, Kargupta K, Bhaumik J (2005) Electric field induced instability and pattern formation in thin liquid films. *Langmuir* 21:3710–3721.
- Morariu MD, et al. (2003) Hierarchical structure formation and pattern replication induced by an electric field. *Nat Mater* 2:48–52.
- Bhat P, et al. (2010) Formation of beads-on-a-string structures during break-up of viscoelastic filaments. *Nat Phys* 6:625–631.
- Oliveira MSN, McKinley GH (2005) Iterated stretching and multiple beads-on-a-string phenomena in dilute solutions of highly extensible flexible polymers. *Phys Fluids* 17:071704.
- Goldin M, Yerushalmi H, Pfeffer R, Shinnar R (1969) Breakup of a laminar capillary jet of a viscoelastic fluid. *J Fluid Mech* 38:689–711.
- Park JU, et al. (2007) High-resolution electrohydrodynamic jet printing. *Nat Mater* 6:782–789.
- Collins RT, Jones JJ, Harris MT, Basaran OA (2008) Electrohydrodynamic tip streaming and emission of charged drops from liquid cones. *Nat Phys* 4:149–154.
- Yu JH, Fridrikh SV, Rutledge GC (2006) The role of elasticity in the formation of electrospun fibers. *Polymer* 47:4789–4797.
- Ferraro P, Coppola S, Grilli S, Paturzo M, Vespini V (2010) Dispensing nano-pico droplets and liquid patterning by pyroelectrodynamics shooting. *Nat Nanotechnol* 5:429–435.
- Dickey MD, et al. (2006) Novel 3-D structures in polymer films by coupling external and internal fields. *Langmuir* 22:4315–4318.
- Garcés-Chávez V, McGloin D, Melville H, Sibbett W, Dholakia K (2002) Simultaneous micromanipulation in multiple planes using a self reconstructing light beam. *Nature* 419:145–147.
- Armani AM, et al. (2007) Label-free, single-molecule detection with optical microcavities. *Science* 317:783–787.
- Vollmer F, Arnold S, Keng D (2008) Single virus detection from the reactive shift of a whispering-gallery mode. *Proc Natl Acad Sci USA* 105:20701–20704.
- Francois A, Himmelhaus M (2009) Whispering gallery mode biosensor operated in the stimulated emission regime. *Appl Phys Lett* 94:031101.
- Beier HT, Coté GL, Meissner KE (2009) Whispering gallery mode biosensors consisting of quantum dot-embedded microspheres. *Ann Biomed Eng* 37:1974–1983.
- Haase J, et al. (2010) Hemispherical resonators with embedded nanocrystal quantum dot emitters. *Appl Phys Lett* 97:211101.
- Dong CH, et al. (2009) Fabrication of high-Q polydimethylsiloxane optical microspheres for thermal sensing. *Appl Phys Lett* 94:231119.
- Ioppolo T, Ayaz U, Ötügen MW (2009) Tuning of whispering gallery modes of spherical resonators using an external electric field. *Opt Express* 17:16465–16479.
- Sill TJ, von Recum HA (2008) Electrospinning: Applications in drug delivery and tissue engineering. *Biomaterials* 29:1989–2006.
- Rosenblum B, Braunlich P, Carrico JP (1974) Thermally stimulated field emission from pyroelectric LiNbO $_3$ . *Appl Phys Lett* 25:17–19.